

Online Algorithms for Hierarchical Inference in Deep Learning applications at the Edge

VISHNU NARAYANAN MOOTHEDATH, KTH Royal Institute of Technology, Sweden

JAYA PRAKASH CHAMPATI, IMDEA Networks Institute, Spain

JAMES GROSS, KTH Royal Institute of Technology, Sweden

We consider a resource-constrained Edge Device (ED) embedded with a small-size ML model (S-ML) for a generic classification application, and an Edge Server (ES) that hosts a large-size ML model (L-ML). Since the inference accuracy of S-ML is lower than that of the L-ML, offloading all the data samples to the ES results in high inference accuracy, but it defeats the purpose of embedding S-ML on the ED and deprives the benefits of reduced latency, bandwidth savings, and energy efficiency of doing local inference. To get the best out of both worlds, i.e., the benefits of doing inference on the ED and the benefits of doing inference on ES, we explore the idea of Hierarchical Inference (HI), wherein S-ML inference is only accepted when it is correct, otherwise the data sample is offloaded for L-ML inference. However, the ideal implementation of HI is infeasible as the correctness of the S-ML inference is not known to the ED. We thus propose an online meta-learning framework to predict the correctness of the S-ML inference. The resulting online learning problem turns out to be a Prediction with Expert Advice (PEA) problem with continuous expert space. We consider the full feedback scenario, where the ED receives feedback on the correctness of the S-ML once it accepts the inference, and the no-local feedback scenario, where the ED does not receive the ground truth for the classification, and propose the HIL-F and HIL-N algorithms and prove a regret bound that is sublinear with the number of data samples. We evaluate and benchmark the performance of the proposed algorithms for image classification applications using four datasets, namely, Imagenette and Imagewoof [18], MNIST [24], and CIFAR-10 [23].

Additional Key Words and Phrases: hierarchical inference, edge computing, regret bound, continuous experts, expert advice prediction

1 INTRODUCTION

Emerging applications in smart homes, smart cities, intelligent manufacturing, autonomous internet of vehicles, etc., are increasingly using Deep Learning (DL) inference. Collecting data from the Edge Devices (EDs) and performing remote inference in the cloud results in bandwidth, energy, and latency costs as well as reliability (due to wireless transmissions) and privacy concerns. Therefore, performing local inference using embedded DL models, which we refer to as S-ML (Small-ML) models, on EDs has received significant research interest in the recent past [10, 29, 37]. These S-ML models range from DL models that are optimized for moderately powerful EDs such as mobile phones to tinyML DL models that even fit on microcontroller units. However, S-ML inference accuracy reduces with the model size and can be potentially much smaller than the inference accuracy of large-size state-of-the-art DL models, which we refer to as L-ML (Large-ML) models, that can be deployed on Edge Servers (ESs). For example, for an image classification application, an S-ML can be a quantized *MobileNet* [17] with a width multiplier of 0.25, that has a memory size of 0.5 MB and an inference accuracy of 39.5% for classifying ImageNet dataset [9], whereas CoCa [39], an L-ML, has an accuracy of 91% and a memory size in the order of GBs.

One may choose to achieve the accuracy of L-ML model while utilizing the computational capabilities of EDs using the well-known DNN partitioning techniques, e.g., see [20, 21, 25]. Note that such partitioning techniques require

Authors' addresses: Vishnu Narayanan Moothedath, vnmo@kth.se, KTH Royal Institute of Technology, Malvinas Väg 10, Stockholm, Sweden, 10044; Jaya Prakash Champati, jaya.champati@imdea.org, IMDEA Networks Institute, Avda. del Mar Mediterraneo, 22, Madrid, Spain, 28918; James Gross, jamesgr@kth.se, KTH Royal Institute of Technology, Malvinas Väg 10, Stockholm, Sweden, 10044.

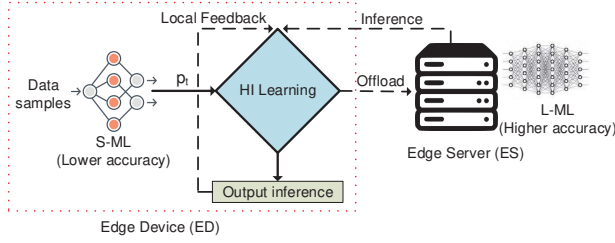


Fig. 1. Schematic of the HI meta-learning framework

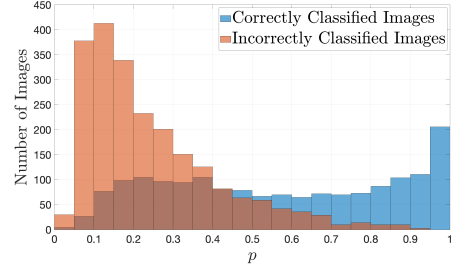


Fig. 2. Classification of Imagenette by a small-size quantized MobileNet using width multiplier 0.25 [17].

processing time and energy profiling of the layers on EDs as well as on ESs to decide the optimal partition points. Early Exit is yet another technique that introduces side branches in between the layers of DL models to trade-off accuracy with latency [34]. In this work, we explore the novel idea of *Hierarchical Inference* (HI) that complements the above techniques for performing DL inference at the edge. Consider that an ED is embedded with an S-ML and an L-ML¹ is deployed on an ES (to which the ED enlists to get help for doing inference). In HI, we propose that an ED first observes the S-ML inference on each data sample and offloads it to L-ML only if S-ML inference is incorrect.

Clearly, the ambition of HI is to maximize the use of S-ML in order to reap the benefits of reduced latency, bandwidth savings, and energy efficiency while not losing inference accuracy by offloading strategically to L-ML, thus achieving the best benefits out of the two worlds: EDs and ESs. However, the central challenge is that the incorrect inferences are inherently unknown at the ED and thus a decision under uncertainty needs to be taken. In this work, we focus on the pervasive *classification applications* and address the above sequential decision problem by proposing a novel HI meta-learning framework, shown in Fig. 1, that facilitates the ED to decide if a current S-ML inference for a given sample should be accepted or the sample to be offloaded. In our framework, for each sample, the HI learning algorithm observes p , the maximum probability value in the probability distribution over classes output by the S-ML. It then decides to offload, receiving a fixed cost $0 \leq \beta < 1$, or not to offload, receiving a cost 0 if the inference is correct, and a cost 1, otherwise. We will show later that this cost structure facilitates HI by maximizing the offloading of samples with incorrect inference and not offloading the samples with correct inference. To simplify the analysis, we assume that S-ML accepts the inference of L-ML as the ground truth implying that the top-1 accuracy of L-ML is 100%. The justification for this assumption is that the ED cannot know the ground truth when L-ML provides incorrect inference and thus by accepting the L-ML inference the ED tries to achieve the top-1 accuracy of L-ML.

Intuitively, if the maximum probability p is high, then accepting S-ML inference will likely result in cost 0 and thus, it is beneficial to do so. However, if p is low, the cost will likely be equal to 1, and thus offloading with cost β is beneficial. This can be seen from Fig. 2, where we present the number of misclassified and correctly classified images of the dataset *Imagenette* [18] by the classifier *MobileNet* [17]. Observe that, for $p \geq 0.45$ (approximately) there are more images correctly classified. Thus offloading for images with $p < 0.45$ might look like a reasonable policy, where the images that statistically tend to be correctly classified are processed locally and those that are not are offloaded. In this work, we design learning algorithms that learn the best threshold $\theta \in [0, 1)$ with performance guarantees after

¹Both S-ML and L-ML are trained ML models deployed for providing inference and HI does not modify these models.

assigning quantifiable cost functions. Using these algorithms in each step, we decide to offload if $p < \theta$ and not offload, otherwise.

The above problem falls in the domain of Prediction with Expert Advice (PEA) [6]. However, we have continuous expert space (or action space) for θ and therefore, as explained later in Section 4, the standard Exponentially Weighted average Forecaster (EWF) does not have a regret bound for our problem. Another challenge is that, in the case of accepting S-ML inference, the local cost is not observable as the ED will not know if the inference is correct or not; we call this *no-local feedback* scenario. To tackle this challenge, we first design an algorithm for the important scenario where local feedback is available – for example, a human user providing this feedback. We refer to this as *full feedback* scenario. We then extend the algorithm to the no-local feedback scenario.

A novel aspect of our algorithms is that they use the structural properties of the HI learning problem at hand to find a set non-uniform intervals obtained by doing dynamic and non-uniform discretizations, and use these intervals as experts, there by transforming the problem from a continuous to a discrete domain without introducing any error due to this discretization. To the best of our knowledge, our work is the first attempt to extend the concept of continuous experts to the no-local feedback scenario and find regret bounds for the same. We summarize our main contributions below.

- We propose a novel meta-learning framework for HI that decides whether a data sample that arrived should be offloaded or not based on S-ML output. For the full feedback scenario, we prove that $O(\sqrt{n \log n})$ is the lower bound for the regret that can be achieved by any randomized algorithm for a general loss function, where n is the number of data samples.
- We propose the HI Learning with Full feedback (HIL-F) algorithm that uses exponential weighting and dynamic non-uniform discretization. We prove that HIL-F has $\sqrt{n \ln(1/\lambda_{\min})}/2$ regret bound, where λ_{\min} is the minimum difference between any two **distinct** p values among the n samples.
- We propose HI Learning with the no-local feedback (HIL-N) algorithm, which on top of HIL-F, uses an unbiased estimate of the loss function. We prove a regret bound $O(n^{2/3} \ln^{1/3}(1/\lambda_{\min}))$. We discuss the ways to approximate λ_{\min} and find the optimal values of the parameters used.
- We show that the computational complexity of our algorithms in round t is $O(\min(t, \frac{1}{\lambda_{\min}}))$.
- Finally, we evaluate the performance of the proposed algorithms for image classification application using four datasets, namely, Imagenette and Imagewoof [18], MNIST [24], and CIFAR-10 [22, 23]. For Imagenette and Imagewoof we use MobileNet, for MNIST we implement a linear classifier for S-ML, and for CIFAR-10, we use a readily available CNN. We compare with four baseline algorithms – the optimal fixed- θ policy, one that offloads all samples, one that does not offload any, and a hypothetical genie algorithm that knows the ground truth.

This paper is organized as follows: In Section 2 we go through the related research and explain the novelty in the contributions. In Section 3, we describe the system model followed by some background information and preliminary results in Section 4. Sections 5 and 6 details HIL-F and HIL-N, derive their regret bounds, and Section 7 discuss their computational complexity. Finally, we show the numerical results in Section 8 and conclude in Section 9.

2 RELATED WORK

Inference Offloading: Since the initial proposal of edge computing in [30], significant attention was given to the computational offloading problem, wherein the ED needs to decide which jobs to offload and how to offload them to an ES. The majority of works in this field studied offloading generic computation jobs, e.g., see [8, 15, 32]. In contrast, due

to the growing interest in edge intelligence systems, recent works studied offloading data samples for ML inference both from a theoretical [12, 26, 27] and practical [35, 36] perspectives. In [27], offloading between a mobile device and a cloud is considered. The authors account for the time-varying communication times by using model selection at the cloud and by allowing the duplication of processing the job at the mobile device. In [12], the authors considered a scalable-size ML model on the ED and studied the offloading decision to maximize the total inference accuracy subject to a time constraint. All the above works focus on dividing the load of the inference and do not consider HI and online learning. Our work is in part motivated by [26], where the authors assumed that the energy consumption for local inference is less than the transmission energy of a sample and studied offloading decision based on a confidence metric computed from the probability distribution over the classes. However, in contrast to our work, the authors do not consider the meta-learning framework and compute a threshold for the confidence metric based on the energy constraint at the ED.

On-Device Inference. Several research works focused on designing S-ML models to be embedded on EDs that range from mobile phones to microcontroller units. While optimization techniques such as parameter pruning and sharing [16], weights quantization [28], and low-rank factorization [11] were used to design the S-ML models, techniques such as EarlyExit were used to reduce the latency of inference. For example, [38] studied the use of DNNs with early exits [34] on the edge device, while [33] studied the best DNN selection on the edge device for a given data sample to improve inference accuracy and reduce latency. These works do not consider inference offloading and in turn HI.

DNN Partitioning: Noting that mobile devices such as smartphones are embedded with increasingly powerful processors and the data that needs to be transmitted between intermediate layers of a DNN is much smaller than the input data in several applications, the authors in [21] studied partitioning DNN between a mobile device and cloud to reduce the mobile energy consumption and latency. Following this idea, significant research work has been done that includes DNN partitioning for more general DNN structures under different network settings [19, 25] and using heterogeneous EDs [20], among others. In contrast to DNN partitioning, under HI, ED, and ES may import S-ML and L-ML algorithms from the pool of trained ML algorithms available on open-source libraries such as Keras, TFLite, and PyTorch. Furthermore, HI doesn't even require that S-ML and L-ML be DL models but rather they can even be signal processing algorithms. On the one hand, there is significant research by the tinyML community for building small-size DNNs that can be embedded on microcontrollers and also in designing efficient embedded hardware accelerators [29]. On the other hand, abundant state-of-the-art DNNs are available at edge servers that provide high inference accuracy. Our work is timely as HI will equip ML at the edge to reap the benefits of the above two research thrusts. To the best of our knowledge, we are the first to propose an online meta-learning framework for HI.

Online Learning: The problem of minimizing the regret, when the decision is chosen from a finite expert space falls under the well-known Prediction with Expert Advice (PEA) or Multi-Armed Bandit (MAB) problems [3, 6]. We will explain more about these problems in Section 4. We will see that we cannot directly use these problems due to the uncountable nature of the expert space in our problems which we will elaborate in 3. We will also explain why some of the existing literature on continuous extensions of PEA and MAB are not suited or sub-optimal for our specific problem.

3 SYSTEM MODEL AND PROBLEM STATEMENT

We consider the system shown in Fig. 1, with an ED enlisting the service of an ES for data classification applications. For the EDs, we focus on resource-constrained devices such as IoT sensors or microcontroller units. The ED is embedded with an S-ML which provides lower *inference accuracy*, i.e., the top-1 accuracy, whereas the ES runs an L-ML with higher accuracy. For example, for an image classification application, an S-ML can be a quantized MobileNet [17] with a width multiplier of 0.25; its memory size is 0.5 MB and has an inference accuracy of 39.5% for classifying ImageNet dataset [9], whereas CoCa [39], an L-ML, has accuracy 91% and has memory size in the order of GBs. Note that the only assumption that we make on the algorithms is that the L-ML is significantly more accurate and costlier than the S-ML. Thus, we do not specify what exactly the S-ML or the L-ML algorithms needs to be, but can be any classification algorithm including regression algorithms, SVMs, random forests, and DNNs. Given an arbitrary sequence of n data samples that arrive over time at the ED, the question we study is: For each sample, should the ED offload for inference from L-ML or accept the inference from S-ML? We approach this as an online sequential decision problem. We assume that each sample first goes through local inference and the decision is made according to the inference results and parameters. Note that this is an essential assumption to facilitate HI, otherwise, the ED cannot infer anything about the sample. Also, as argued earlier in Section 1, we assume that all the offloaded images will be correctly classified by the L-ML. This assumption is not necessary for the proposed algorithms, but since the ED cannot possibly know if the inference provided by the ES is correct or wrong, we use the assumption to simplify the formulation.

Let t denote the index of a data sample (e.g., an image), or simply sample, that arrives t -th in the sequence. Let p_t denote the maximum probability in the probability distribution over the classes output by S-ML for the sample t .² Note that the class corresponding to p_t is declared as the true class for computing the top-1 accuracy. Intuitively speaking, p_t is the confidence level of S-ML for classifying sample t and it is a natural candidate to use for HI. Let binary random variable Y_t denote the cost representing the ground truth that is equal to 0 if the class corresponding to p_t is the correct class and is equal to 1, otherwise. Clearly, given an S-ML model, Y_t depends on p_t and the sample. Let $\beta \in [0, 1)$ denote the cost incurred for offloading the image for inference at the ES. This cost, for example, may include the costs for the transmission energy and the idle energy spent by the transceiver till the reception of the inference. Note that, if $\beta \geq 1$, then accepting the inference of S-ML, which incurs a cost at most 1, for all samples will minimize the total cost.

If the ED offloads sample t , it incurs cost β , and if it accepts the S-ML inference, it incurs a cost Y_t . In the latter case, the ED may not know Y_t , in general, and we refer to it by *no-local feedback* scenario. If Y_t is revealed once the ED accepts S-ML, we refer to by *full feedback* scenario. In either scenario, if the ED offloads and receives the inference from the ES, it can use that inference to infer Y_t . As explained in Section 1, in round t , we use the following decision rule \mathfrak{D}_t based on the choice of threshold $\theta_t \in [0, 1]$:

$$\mathfrak{D}_t = \begin{cases} \text{Do not offload} & \text{if } p_t \geq \theta_t, \\ \text{Offload} & \text{if } p_t < \theta_t. \end{cases} \quad (1)$$

²Note that, in a classification application, a classifier typically outputs a probability distribution over the classes. Our framework allows other metrics, besides p_t , that are computed based on the probability distribution over classes.

Therefore, given p_t , choosing threshold θ_t results in a cost/loss $l(\theta_t, Y_t)$ at step t , given by

$$l(\theta_t, Y_t) = \begin{cases} Y_t & p_t \geq \theta_t, \\ \beta & p_t < \theta_t. \end{cases} \quad (2)$$

Note that, we omit the variable p_t from the loss function $l(\theta_t, Y_t)$ for notational simplicity. We focus on designing online algorithms that learn the best threshold, which balances the conflicting objectives of reducing the number of images offloaded and increasing the inference accuracy, thereby improving the responsiveness and energy efficiency of the system.

We use boldface notations to denote vectors. Let $Y_t = \{Y_\tau\}$, $\theta_t = \{\theta_\tau\}$, and $\mathbf{p}_t = \{p_\tau\}$, $\tau = 1, 2, \dots, t \leq n$. Further, let $Y := Y_n$, $\theta := \theta_n$ and $\mathbf{p} := \mathbf{p}_n$ for convenience. Finally, we define λ_{\min} as the minimum difference between any two distinct probability values in the sequence \mathbf{p}_n . Define the cumulative cost $L(\theta, Y)$ as $L(\theta, Y) = \sum_{t=1}^n l(\theta_t, Y_t)$. Also let $\theta^* = \{\theta^*, \theta^*, \dots\}$, a vector of size n with all values θ^* , denote an optimal fixed- θ policy and $L(\theta^*, Y)$ denote the corresponding cost. Then,

$$L(\theta^*, Y) = \sum_{t=1}^n l(\theta^*, Y_t),$$

where θ^* need not necessarily be unique and is given by

$$\theta^* = \arg \min_{\theta \in [0,1]} \sum_{t=1}^n l(\theta, Y_t).$$

Given a sequence Y , we now define the regret under an arbitrary algorithm π as

$$R_n = \mathbb{E}_\pi [L(\theta, Y)] - L(\theta^*, Y), \quad (3)$$

where the expectation $\mathbb{E}_\pi[\cdot]$ is with respect to the distribution induced by π .

In this work, we are interested finding algorithms for both the full feedback and no-local feedback scenarios that have a sublinear upper bound (i.e., a bound that goes to 0 as n goes to ∞) on $\mathbb{E}_Y[R_n]$ – the expected regret over the distribution of all possible sequences Y . We call this bound an expected regret bound and note that if we can find a regret bound that is applicable for any given sequence Y , the same bound is also applicable for the expected regret (or even the maximum regret) over all possible sequences of Y . For this reason, and for the sake of simplicity, we will only carry out the analysis for a given Y in the upcoming analysis sections. However, later in the numerical section, we will show the results with expected average regret $\mathbb{E}_Y[\frac{1}{n}R_n] = \frac{1}{n}\mathbb{E}_Y[R_n]$ and expected average cost $\frac{1}{n}\mathbb{E}_{Y,\pi}[L(\theta, Y)]$. We take the average over the number of samples n to remove the dependency on the size of different datasets and normalize the maximum to 1, for easy comparison.

Before going to the next section, we summarize the abbreviations and notations used in this paper in TABLE 1 below.

ED	edge device	HI	hierarchical inference	HIL-F	HIL algorithm: full feedback
ES	edge server	HIL	hierarchical inference learning	HIL-N	HIL algorithm: no-local feedback
S-ML	small-size ML	PEA	prediction with expert advice	EWf	exponentially weighted forecaster
L-ML	large-size ML	$p_{[i]}$	i^{th} smallest district value in the set of available probabilities $\{p_1, p_1, \dots\}$		

Table 1. Table of abbreviations.

4 BACKGROUND AND PRELIMINARY ANALYSIS

Learning Problems: The HI learning problem falls into the category of PEA [6] problems. In the standard PEA problem, N experts (or actions) are available for a predictor – known formally as a *forecaster*. When the forecaster chooses an expert, it receives a cost/reward corresponding to that expert. If the cost is only revealed for the chosen expert, then this setting is the MAB. In contrast to the standard PEA, we have an uncountable expert space where the expert θ_t belongs to the continuous space $[0, 1]$. Continuous action space is well studied in MAB settings, e.g., see [1, 4, 31], where the main technique used is to discretize the action space and bound the regret by assuming that the unknown loss function has smoothness properties such as uniformly locally Lipschitz. However, the problem at hand does not assume any smoothness properties for the loss function.

As discussed briefly in Section 1, one well-known forecaster for standard PEA is the exponential weighted average forecaster (EWF). For each expert, EWF assigns a weight that is based on the cost incurred for choosing this expert. For each prediction, EWF selects an expert with a probability computed based on these weights. It is known that for n predictions, EWF achieves a regret $\sqrt{n \ln N}/2$. However, the continuous nature of the expert space renders EWF not directly applicable for solving the problem at hand and we need an extension of EWF. Such an extension was considered in [2], and a regret bound for convex losses is obtained for continuous experts, conditioned on a hyperparameter $\gamma > 0$. Later, a particular γ is proposed to get the optimum regret bound of $1 + \sqrt{n \ln n}/2$. We, on the other hand, do not require any hyperparameter and more importantly do not assume any convexity for the loss function. In addition, [2] does not describe how to compute the integral required for computing the weights. Furthermore, the solution in [2] is only applicable to HIL-F with full feedback, but not to HIL-N in which case ours is the first work to the best of our knowledge.

One may discretize $[0, 1]$ with a uniform interval length Δ and use the standard EWF, where a straightforward substitution of the number of experts $N = 1/\Delta$ results in regret bound $\sqrt{n \ln(1/\Delta)}/2$. However, to not sacrifice the accuracy due to this discretization, one has to take Δ small enough such that no two probability realization p_t falls within an interval. This is to make sure that the cumulative loss function is constant within each interval, which will be more clear after Lemma 4.1. Thus, if λ_{\min} is the minimum separation between any two distinct probabilities $p_t, 1 \leq t \leq n$, the best attainable regret bound of a standard EWF using uniform discretization is $\sqrt{n \ln(1/\lambda_{\min})}/2$ with $N = 1/\lambda_{\min}$. We will soon see that these regret bounds are similar to what we get using our proposed algorithms, but the added complexity with a large number of experts from the first round onwards makes it suboptimal.

In this paper, we start with the continuous experts and then use the structure of the problem to formulate it in a discrete domain. We propose a non-uniform discretization that retains the accuracy of a continuous expert while reducing the complexity to the theoretical minimum with at most $n + 1$ experts after n^{th} round. Note that, due to the non-uniform discretization, the proposed HIL does not involve Δ , but instead involves λ_{\min} , where $1/\lambda_{\min}$ acts similar to N in the regret bound. In Section 5, we provide simple methods to approximate λ_{\min} .

Preliminary Analysis: In order to choose a good threshold θ_t in round t , we take a hint from the discrete PEA [6] where a weight for an expert is computed using the exponential of the scaled cumulative losses incurred for potentially

choosing that expert. We extend this idea and define continuous weight function $w_t(\theta)$ as follows:

$$\begin{aligned} w_{t+1}(\theta) &= e^{-\eta \sum_{\tau=1}^t l(\theta, Y_\tau)} \\ &= e^{-\eta \sum_{\tau=1}^{t-1} l(\theta, Y_\tau)} e^{-\eta l(\theta, Y_t)} = w_t(\theta) e^{-\eta l(\theta, Y_t)}. \end{aligned} \quad (4)$$

$$W_{t+1} = \int_0^1 w_{t+1}(\theta) d\theta. \quad (5)$$

Here, $\eta > 0$ is the learning rate. At each round t , the normalized weights give the probability distribution for choosing the next threshold θ_{t+1} , and thus they can be used to learn the system. However, it comes with two challenges – (i) finding a (set of) thresholds that follow this distribution, and (ii) computing the integral. Although these challenges can be solved using direct numerical methods, they incur a large amount of computational cost. For instance, the inverse transformation method can generate a random sample of the threshold with this distribution. Instead, we use the facts from (1) and (2) that our final decision (to offload or not) depends solely on the relative position of θ_t and p_t , but not directly on θ_t . Thus, using the distribution given by the normalized weights, we define q_t as the probability of *not* offloading, i.e., the probability that θ_t is less than p_t , where

$$q_t = \frac{\int_0^{p_t} w_t(x) dx}{W_t}. \quad (6)$$

Thus, the decision \mathfrak{D}_t from (1) boils down to *do not offload* and *offload* with probabilities q_t and $(1 - q_t)$, respectively.

With the first challenge mitigated, we look for efficient methods to compute the integral in (6). Note that the cumulative loss function $L(\theta_t, Y_t) = \sum_{\tau=1}^t l(\theta_\tau, Y_\tau)$ can take potentially 3^t different values (because of 0, 1, or β cost in each step), without any necessary pattern, and hence direct analytical integration is not possible. To address this issue, we leverage the result of the following lemma (Lemma 4.1) and convert the integral into summation by discretizing the domain $[0, 1]$ of the integral into a finite set of non-uniform intervals.

The non-uniform discretization suggested by this lemma is incremental and a new interval is (potentially) added in each round. Let's look at the structure of the weight function after n rounds. Let $p_0 = 0$ and $p_N = 1$, where N is the number of intervals formed in $[0, 1]$ by the sequence of probabilities \mathbf{p}_n . Here, we have $N \leq n + 1$ because of the repeated probabilities that do not result in the addition of a new interval. We denote these intervals by $B_i = (p_{[i-1]}, p_{[i]})$, $1 \leq i \leq N$, where $p_{[i]}$ denotes the i -th smallest distinct probability in \mathbf{p}_n . Let m_i , $1 \leq i \leq N$ be the number of times $p_{[i]}$ is repeated in \mathbf{p}_n . For instance, $N = n + 1$ and $p_{[i]} = p_i$ iff $m_i = 1 \forall i$. Finally, let $Y_{[i]}$, $i = 1, 2, \dots, n$ be the i -th element in the ordered set of local inference costs ordered according to the increasing values of the corresponding probability p_i . Note that, i in $Y_{[i]}$ goes up to n while i in $p_{[i]}$ goes only up to N because any two local inference costs Y_j and Y_k associated with repeated probability values $p_j = p_k$ are two different but i.i.d random variables.

LEMMA 4.1. *The function $L(\theta, Y)$ is a piece-wise constant function with a constant value in each interval B_i . Furthermore, if there are no repetitions in the sequence \mathbf{p}_n , then*

$$L(\theta^*, Y) = \min_{1 \leq i \leq n+1} \left\{ (i-1)\beta + \sum_{k=i}^n Y_{[k]} \right\}.$$

PROOF. By definition, p_t falls on the boundary of B_i , $\forall t$, for some i . Hence, B_i is a subset of either $(0, p_t]$ or $(p_t, 1]$.

$$\Rightarrow l(\theta_t, Y_t) = \begin{cases} Y_t, & \forall \theta : \theta_t \in B_i \subset (0, p_t], \text{ and} \\ \beta, & \forall \theta : \theta_t \in B_i \subset (p_t, 1]. \end{cases} \quad (7)$$

Thus, $\forall i \leq N$, $l(\theta, Y_t) := l(B_i, Y_t), \forall \theta \in B_i$. That is, the cost for all θ within an interval B_i takes a constant value of $l(B_i, Y_t)$, and this value depends on whether $p_{[i]}$ (the upper boundary of B_i) is greater than p_t or not. To prove the second part, note that $L(\theta, Y) = \sum_{t=1}^n l(B_i, Y_t) : \theta \in B_i$.

$$\begin{aligned} \Rightarrow L(\theta^*, Y) &= \min_{\theta \in [0,1]} L(\theta, Y) = \min_{1 \leq i \leq N} \sum_{t=1}^n l(B_i, Y_t). \\ \sum_{t=1}^n l(B_i, Y_t) &= \sum_{t=1}^n [\beta \mathbb{1}(p_t < p_{[i]}) + Y_t \mathbb{1}(p_t \geq p_{[i]})] \\ &= \beta \sum_{j=1}^{i-1} m_j + \sum_{k=1+\sum_{j=1}^{i-1} m_j}^n Y_{[k]} \\ \Rightarrow L(\theta^*, Y) &= \min_{1 \leq i \leq N} \left\{ \beta \sum_{j=1}^{i-1} m_j + \sum_{k=1+\sum_{j=1}^{i-1} m_j}^n Y_{[k]} \right\} \end{aligned} \quad (8)$$

When there are no repetitions, we can substitute $m_j = 1, \forall j$ in the above expression to complete the proof. \square

From Lemma 4.1, we infer that for any t the weight function is constant within the intervals defined by p_t , and we can compute the integral in (6) by adding multiple rectangular areas formed by the length of each interval B_i and the corresponding constant weight within it. Thus, by converting the integral of $w_t(\theta)$ in a continuous domain to a summation of areas of rectangles with non-uniform bases, we not only reduce the complexity but also do that without sacrificing the accuracy of the results. We will discuss more on the computational complexity in Section 7. Note that the property of the piece-wise nature – given by the first part of Lemma 4.1 – is not only valid for the particular loss function $l(\theta_t, Y_t)$, but also for any other loss function with a single decision boundary (as in (2)) and discrete costs on either side of this boundary. This becomes important when we use a modified loss function for finding the optimum decision boundary θ^* later in Section 6.

Consider the scenario where p_n is known a priori. We can then use the standard EWF with N intervals with the cost corresponding to interval B_i as defined in (7). The following Corollary states the regret bound for this algorithm.

COROLLARY 4.2. *If the sequence p_n is known a priori, an EWF that uses the intervals B_i as experts achieves $\sqrt{n \ln N/2}$ regret bound. Consequently, given that $N = O(n)$, the regret bound of EWF is $O(\sqrt{n \ln n})$.*

Note that, for the standard PEA with N experts, $\sqrt{n \ln N/2}$ is the lower bound for the regret for any randomized algorithm [5]. Thus, Corollary 4.2 implies that for the problem at hand, under a general loss function, no randomized algorithm has regret bound lower than $O(\sqrt{n \ln n})$. Clearly, the lower bound $O(\sqrt{n \ln n})$ is much higher than the lower bound of PEA, where the number of experts is independent of n . This establishes the hardness of our problem. Adding to the difficulty, $O(\sqrt{n \ln n})$ can only be achieved if p_n is known a priori, which is not the case in practice.

With all preliminaries covered, we now present the HIL algorithms and their regret bounds for full feedback and no-local feedback scenarios in Sections 5 and 6, respectively.

5 FULL FEEDBACK

In this section, we consider the full-feedback scenario, where the algorithm receives the ground truth Y_t for all the samples, including those that are not offloaded by accepting the S-ML inference. For this scenario, we present the HIL-F algorithm in Algorithm 1. Some algorithmic rules for the parameter updates are given later in Section 7. As explained in the previous section, given p_t , we compute q_t , the probability to not offload. Once the decision is made using q_t , the costs are received and the weights are updated using (4) and (5). For simplicity, we denote the expected cost received by HIL-F in round t by $\bar{l}(\theta_t, Y_t)$ and is given by

$$\bar{l}(\theta_t, Y_t) = \mathbb{E}_{Q_t}[l(\theta_t, Y_t)] = Y_t q_t + \beta(1 - q_t),$$

where the expectation is with respect to the probability distribution dictated by q_t . Also, let $\bar{L}(\theta, Y) = \sum_{t=1}^n \bar{l}(\theta_t, Y_t)$ denote the total expected cost after n rounds. In the theorem below, we provide a regret bound for HIL-F.

THEOREM 5.1. *For $\eta > 0$, HIL-F achieves the following regret bound:*

$$R_n = \bar{L}(\theta, Y) - L(\theta^*, Y) \leq \frac{1}{\eta} \ln \frac{1}{\lambda_{\min}} + \frac{n\eta}{8}.$$

PROOF. Recall from Lemma 4.1 that $p_{[i]}, B_i = (p_{[i-1]}, p_{[i]})$, and $l(B_i, Y_t)$ are the i -th smallest probability, intervals formed by them, and the constant loss function within that interval at round t , respectively. Also, $\lambda_i = p_{[i]} - p_{[i-1]}$ and $N \leq n + 1$ correspond to the length of the intervals i and the total number of intervals, respectively. Finally, $\lambda_{\min} = \min_{1 \leq i \leq N} \lambda_i$. Substituting $t = 0$ in (5), we have $W_1 = 1$. Thus, taking logarithm of $\frac{W_{n+1}}{W_1}$ gives,

$$\begin{aligned} \ln \frac{W_{n+1}}{W_1} &= \ln \int_0^1 e^{-\eta \sum_{t=1}^n l(x, Y_t)} dx \\ &= \ln \sum_{i=1}^N \lambda_i e^{-\eta \sum_{t=1}^n l(B_i, Y_t)} \\ &\geq \ln \max_{1 \leq i \leq N} \left(\lambda_{\min} e^{-\eta \sum_{t=1}^n l(B_i, Y_t)} \right) \\ &= -\eta \min_{1 \leq i \leq N} \sum_{t=1}^n l(B_i, Y_t) - \ln \frac{1}{\lambda_{\min}} \\ &= -\eta \min_{\theta \in [0,1]} \sum_{t=1}^n l(\theta, Y_t) - \ln \frac{1}{\lambda_{\min}}. \end{aligned} \tag{9}$$

Now, we bound the ratio $\frac{W_{t+1}}{W_t}$.

$$\begin{aligned} \ln \left(\frac{W_{t+1}}{W_t} \right) &= \ln \left(\frac{\int_0^1 w_{t+1}(x) dx}{W_t} \right) \\ &= \ln \left(\int_0^1 \frac{w_t(x)}{W_t} e^{-\eta l(x, Y_t)} dx \right). \end{aligned}$$

By using Hoeffding's lemma³ in the above equation, we get

Algorithm 1: The HIL-F algorithm for full feedback.

- 1: Initialize: Set $w_1(\theta) = 1, \forall \theta \in [0, 1]$ and $N = 1$.
 - 2: **for** every sample in round $t = 1, 2, \dots$ **do**
 - 3: S-ML outputs p_t .
 - 4: Compute q_t using (5) and (6), and generate Bernoulli random variable Q_t with $\mathbb{P}(Q_t = 1) = q_t$.
 - 5: **if** $Q_t = 1$ **then**
 - 6: Accept the S-ML inference and receive cost Y_t .
 - 7: **else**
 - 8: Offload the sample and receive cost β .
 - 9: **end if**
 - 10: Find the loss function using (2).
 - 11: **if** p_t is not a repetition **then**
 - 12: Update the intervals by splitting the interval containing p_t , at p_t . Increment N by 1.
 - 13: **end if**
 - 14: Update the weights for all intervals using (4), based on the interval positions with respect to p_t .
 - 15: **end for**
-

$$\begin{aligned}
 \ln\left(\frac{W_{t+1}}{W_t}\right) &\leq -\eta \int_0^1 \frac{w_t(x)}{W_t} l(x, Y_t) dx + \frac{\eta^2}{8} \\
 &= -\eta \int_0^{p_t} \frac{w_t(x)}{W_t} l(x, Y_t) dx - \eta \int_{p_t}^1 \frac{w_t(x)}{W_t} l(x, Y_t) dx + \frac{\eta^2}{8} \\
 &= -\eta \left(Y_t \int_0^{p_t} \frac{w_t(x)}{W_t} dx + \beta \int_{p_t}^1 \frac{w_t(x)}{W_t} dx \right) + \frac{\eta^2}{8}.
 \end{aligned}$$

In the above step, we used (2). Now using (6) to replace the integrals, we get

$$\begin{aligned}
 \ln\left(\frac{W_{t+1}}{W_t}\right) &\leq -\eta (Y_t q_t + \beta(1 - q_t)) + \frac{\eta^2}{8} \\
 &= -\eta \bar{l}(\theta_t, Y_t) + \frac{\eta^2}{8}.
 \end{aligned} \tag{10}$$

Extending this expression telescopically, we get

$$\begin{aligned}
 \ln\left(\frac{W_{n+1}}{W_1}\right) &= \ln\left(\prod_{t=1}^n \frac{W_{t+1}}{W_t}\right) = \sum_{t=1}^n \ln \frac{W_{t+1}}{W_t} \\
 &\leq \sum_{t=1}^n \left[-\eta \bar{l}(\theta_t, Y_t) + \frac{\eta^2}{8} \right] = -\eta \sum_{t=1}^n \bar{l}(\theta_t, Y_t) + \frac{n\eta^2}{8}.
 \end{aligned} \tag{11}$$

Using (9) and (11), we obtain

$$\begin{aligned}
 -\eta \min_{\theta \in [0,1]} \sum_{t=1}^n l(\theta, Y_t) - \ln \frac{1}{\lambda_{\min}} &\leq -\eta \sum_{t=1}^n \bar{l}(\theta_t, Y_t) + \frac{n\eta^2}{8} \\
 \Rightarrow \bar{L}(\theta, Y) &\leq L(\theta^*, Y) + \frac{1}{\eta} \ln \frac{1}{\lambda_{\min}} + \frac{n\eta}{8} \\
 \Rightarrow R_n &\leq \frac{1}{\eta} \ln \frac{1}{\lambda_{\min}} + \frac{n\eta}{8}.
 \end{aligned}$$

³For a bounded random variable $X \in [a, b]$, $\ln(\mathbb{E}[e^{sX}]) \leq s\mathbb{E}[X] + \frac{s^2(b-a)^2}{8}$.

In the last two steps above, we rearranged the terms and divided them with η . □

Here, η is the learning rate of the algorithm. To find η^* , the η that minimizes the above regret bound, we differentiate the regret R_η above to obtain

$$\eta^* = \sqrt{\frac{8 \ln(1/\lambda_{\min})}{n}}. \quad (12)$$

What remains is to find an approximation for λ_{\min} , which is possible through various methods. For instance, one can use the precision of the probability outputs, i.e., if the probability outputs are truncated to 6 decimal places, then we know that $\lambda_{\min} \geq 10^{-6}$. Further, some datasets and/or S-ML models come with specific λ_{\min} . For example, the probability output by MobileNet on the Imagenette dataset is 8-bit and hence the probabilities are integer multiples of $1/256$. Even in cases where all these methods fail, we see that a decent approximation for λ_{\min} is $\hat{\lambda}_{\min} = 1/(n+1)$.

6 NO-LOCAL FEEDBACK

Under no-local feedback, the cost is unknown once the inference of the S-ML is accepted. For this scenario, we use the randomization idea used for label efficient prediction problem [7], which is a variant of the PEA, where the costs in each round are not revealed, unless they are inquired for, and there can only be at most m inquires that can be made. For this variant, EWF is modified as follows: in each round, a Bernoulli random variable Z is generated with probability ϵ . If $Z = 1$, then feedback is requested and the costs are revealed. However, for our problem, the algorithm for the label-efficient prediction problem is not applicable due to the aspect of continuous expert space. Further, we do not have the notion of inquiring about the costs at the ED. Instead, when $Z = 1$, the sample has to be offloaded to the ES with cost β irrespective of the original decision made using q_t . These samples provide the ED with the inference using which the ED computes the cost Y_t .

To address the above aspects we follow the design principles of HIL-F and use non-uniform discretization of the continuous domain and propose the HI algorithm for no-local feedback (HIL-N), which is presented in Algorithm 2. Even though HIL-N and HIL-F have a similar structure, the design of HIL-N is significantly more involved and has the following key differences with HIL-F. Firstly, in line 5 of Algorithm 2, a Bernoulli random variable Z_t is generated with probability ϵ . If $Z_t = 1$, then the sample is offloaded even if $Q_t = 1$, and thus Y_t is realized in this case. This step is used to control the frequency of additional offloads carried out to learn the ground truth Y_t . Secondly, instead of the loss function, the weights are updated using a *pseudo loss function* $\tilde{l}(\theta_t, Y_t)$ defined as follows:

$$\tilde{l}(\theta_t, Y_t) = \begin{cases} 0 & p_t \geq \theta_t, Z_t = 0; & [\text{Do Not Offload}] \\ \frac{Y_t}{\epsilon} & p_t \geq \theta_t, Z_t = 1; & [\text{Offload}] \\ \beta & p_t < \theta_t. & [\text{Offload}] \end{cases} \quad (13)$$

We also update the equations (4), (5) and (6) as follows:

$$w_{t+1}(\theta) = w_t(\theta) e^{-\eta \tilde{l}_t(\theta, Y_t)}, \quad (14)$$

$$W_{t+1} = \int_0^1 w_{t+1}(\theta) d\theta, \text{ and} \quad (15)$$

$$q_t = \frac{\int_0^{p_t} w_t(x) dx}{W_t}. \quad (16)$$

We emphasize that the pseudo loss function $\tilde{l}(\theta_t, Y_t)$ is used only as part of the HIL-N algorithm, and is not the actual cost incurred by the ED. The actual cost remains unchanged and it depends only on the offloading decision and the correctness of the inference if not offloaded. However, this actual incurred cost or the corresponding loss function $l(\theta_t, Y_t)$ is unknown for the no-local feedback scenario, whenever the sample is not offloaded and the local inference is accepted. This is precisely the reason to introduce the pseudo loss function $\tilde{l}(\theta_t, Y_t)$ which is known in each t , and can be used in the HIL-N algorithm to update the weights. Recall from Section 5 that in HIL-F, the cost incurred and the cost used to update the weights are the same, and the incurred cost is β if and only if $p_t < \theta_t$. However in HIL-N, we use the pseudo cost to update the weights, and thus the actual cost incurred can be equal to β even if $p_t \geq \theta_t$. However, we designed the pseudo-loss function such that

$$\mathbb{E}_Z \left[\tilde{l}(\theta_t, Y_t) \right] = l(\theta_t, Y_t). \quad (17)$$

Therefore, the pseudo loss function is an unbiased estimate of the actual loss function, a fact that we will facilitate our analysis. Further, with the addition of a random variable Q , the regret for HIL-N can be rewritten as

$$R_n = \mathbb{E}_{QZ} [L(\theta, Y)] - L(\theta^*, Y), \quad (18)$$

where $\mathbb{E}_{QZ}[\cdot]$ is expectation with respect to random variables $\{Q_1, Q_2, \dots, Q_n\}$ and Bernoulli random variable Z .

THEOREM 6.1. For $\eta, \epsilon > 0$, HIL-N achieves the regret bound

$$R_n \leq n\beta\epsilon + \frac{n\eta}{2\epsilon} + \frac{1}{\eta} \ln(1/\lambda_{min}).$$

PROOF. Step 1: Since the costs incurred and the loss function used for updating the weights are different under HIL-N, we first find a bound for the difference between the expected total cost received and the expected total cost obtained using $\tilde{l}(\theta_t, Y_t)$. From Algorithm 2, we infer that sample t is offloaded if $Q_t = 0$ or $Q_t = 1$ and $Z_t = 1$, and it is not offloaded only when $Q_t = 0$ and $Z_t = 0$. Therefore, we have

$$\mathbb{E}_{Q_t Z} [l(\theta_t, Y_t)] = \beta[1 - q_t + q_t\epsilon] + q_t(1 - \epsilon)Y_t. \quad (19)$$

From (13), we have

$$\begin{aligned} \tilde{l}(\theta_t, Y_t) &= \frac{Y_t}{\epsilon} \mathbb{1}(\theta_t \leq p_t) \mathbb{1}(Z_t = 1) + \beta \mathbb{1}(\theta_t > p_t) \\ \Rightarrow \mathbb{E}_{Q_t Z} \left[\tilde{l}(\theta_t, Y_t) \right] &= Y_t q_t + \beta(1 - q_t). \end{aligned} \quad (20)$$

From (19) and (20), we obtain

$$\begin{aligned} \mathbb{E}_{Q_t Z} [l(\theta_t, Y_t)] - \mathbb{E}_{Q_t Z} \left[\tilde{l}(\theta_t, Y_t) \right] &= \beta\epsilon q_t - Y_t\epsilon q_t. \\ \Rightarrow \mathbb{E}_{QZ} [L(\theta, Y)] - \sum_{t=1}^n \mathbb{E}_{QZ} \left[\tilde{l}(\theta_t, Y_t) \right] &= \beta\epsilon \sum_{t=1}^n q_t - \epsilon \sum_{t=1}^n Y_t q_t \\ &\leq n\beta\epsilon - \epsilon \sum_{t=1}^n Y_t q_t \\ \Rightarrow - \sum_{t=1}^n \mathbb{E}_{QZ} \left[\tilde{l}(\theta_t, Y_t) \right] &\leq -\mathbb{E}_{QZ} [L(\theta, Y)] + n\beta\epsilon. \end{aligned} \quad (21)$$

In the last step above, we have used $q_t \leq 1$, for all t .

Step 2: Using the same analysis to derive (9), we obtain

$$\ln\left(\frac{W_{n+1}}{W_1}\right) \geq -\eta \min_{\theta \in [0,1]} \sum_{t=1}^n \tilde{l}(\theta, Y_t) - \ln \frac{1}{\lambda_{\min}}$$

Note that, here we have $\tilde{l}(\theta, Y_t)$ instead of $l(\theta, Y_t)$. Now using the fact that the expectation over the minimum is upper bounded by the minimum over expectation, we get

$$\begin{aligned} \Rightarrow \mathbb{E}_Z \left[\ln\left(\frac{W_{n+1}}{W_1}\right) \right] &\geq -\eta \min_{\theta \in [0,1]} \sum_{t=1}^n \mathbb{E}_Z \left[\tilde{l}(\theta, Y_t) \right] - \ln \frac{1}{\lambda_{\min}} \\ \Rightarrow \mathbb{E}_Z \left[\ln\left(\frac{W_{n+1}}{W_1}\right) \right] &\geq -\eta L(\theta^*, Y) - \ln(1/\lambda_{\min}). \end{aligned} \quad (22)$$

Step 3: In the following we find a bound for $\ln\left(\frac{W_{t+1}}{W_t}\right)$.

$$\begin{aligned} \ln\left(\frac{W_{t+1}}{W_t}\right) &= \ln\left(\frac{\int_0^1 w_{t+1}(x) dx}{W_t}\right) \\ &= \ln\left(\int_0^1 \frac{w_t(x)}{W_t} e^{-\eta \tilde{l}(x, Y_t)} dx\right) && \text{(using (14))} \\ &\leq \ln\left(\int_0^1 \frac{w_t(x)}{W_t} \left(1 - \eta \tilde{l}(x, Y_t) + \frac{\eta^2}{2} \tilde{l}(x, Y_t)^2\right) dx\right). \end{aligned}$$

In the above step, we used the fact that $e^{-x} \leq 1 - x + x^2/2$. Rearranging the terms, we get

$$\begin{aligned} \ln\left(\frac{W_{t+1}}{W_t}\right) &= \ln\left(1 + \int_0^1 \frac{w_t(x)}{W_t} \left(-\eta \tilde{l}(x, Y_t) + \frac{\eta^2}{2} \tilde{l}(x, Y_t)^2\right) dx\right) \\ &\leq \int_0^1 \frac{w_t(x)}{W_t} \left(-\eta \tilde{l}(x, Y_t) + \frac{\eta^2}{2} \tilde{l}(x, Y_t)^2\right) dx. \end{aligned}$$

The above step follows from the fact that $\ln(1+x) \leq x$, $\forall x > -1$.

$$\Rightarrow \ln\left(\frac{W_{t+1}}{W_t}\right) \leq \int_0^1 \frac{w_t(x)}{W_t} \left(-\eta \tilde{l}(x, Y_t) + \frac{\eta^2}{2\epsilon} \tilde{l}(x, Y_t)\right) dx. \quad (23)$$

In the last step, we have used the fact that $\tilde{l}(x, Y_t) \in [0, 1/\epsilon]$. Note that the integral above can be rearranged as follows:

$$\begin{aligned} \int_0^1 \frac{w_t(x)}{W_t} \tilde{l}(x, Y_t) dx &= \int_0^{p_t} \frac{w_t(x)}{W_t} \tilde{l}(x, Y_t) dx + \int_{p_t}^1 \frac{w_t(x)}{W_t} \tilde{l}(x, Y_t) dx \\ &= \frac{Y_t}{\epsilon} \mathbb{1}(Z_t = 1) q_t + \beta(1 - q_t). \end{aligned}$$

Therefore, we have

$$\begin{aligned} \mathbb{E}_Z \left[\int_0^1 \frac{w_t(x)}{W_t} \tilde{l}(x, Y_t) dx \right] &= Y_t q_t + \beta(1 - q_t) \\ &= \mathbb{E}_{Q_t, Z} \left[\tilde{l}(\theta_t, Y_t) \right], \end{aligned} \quad (24)$$

where we have used (20). Taking expectation with respect Z on both sides in (23) and then substituting (24),

$$\mathbb{E}_Z \left[\ln\left(\frac{W_{t+1}}{W_t}\right) \right] \leq -\eta \mathbb{E}_{Q_t, Z} \left[\tilde{l}(\theta_t, Y_t) \right] + \frac{\eta^2}{2\epsilon} \mathbb{E}_{Q_t, Z} \left[\tilde{l}(\theta_t, Y_t) \right]$$

Algorithm 2: The HIL-N algorithm

-
- 1: Initialize: Set $w_1(\theta) = 1, \forall \theta \in [0, 1]$ and $N = 1$.
 - 2: **for** $t = 1, 2, \dots$ **do**
 - 3: S-ML outputs p_t .
 - 4: Compute q_t using weights from (14) and (15) and generate Bernoulli random variables Q_t and Z_t with $\mathbb{P}(Q_t = 1) = q_t$ and $\mathbb{P}(Z_t = 1) = \epsilon$.
 - 5: **if** $Q_t = 1$ **and** $Z_t = 0$ **then**
 - 6: Accept the S-ML inference and receive cost Y_t (unknown).
 - 7: **else**
 - 8: Offload the sample and receive cost β .
 - 9: **end if**
 - 10: Find the pseudo loss function using (13).
 - 11: **if** p_t is not a repetition **then**
 - 12: Update the intervals by splitting the interval containing p_t at p_t . Increment N by 1.
 - 13: **end if**
 - 14: Update the weights for all intervals using (14), based on the interval positions with respect to p_t .
 - 15: **end for**
-

$$\leq -\eta \mathbb{E}_{Q_t, Z} [\tilde{l}(\theta_t, Y_t)] + \frac{\eta^2}{2\epsilon}. \quad (25)$$

Above, we used the fact that $\mathbb{E}_{QZ} [\tilde{l}(\theta_t, Y_t)] \leq 1$. Taking summation of (25) over t , we obtain

$$\begin{aligned} \mathbb{E}_Z \left[\ln \prod_{t=1}^n \left(\frac{W_{t+1}}{W_t} \right) \right] &\leq -\eta \sum_{t=1}^n \mathbb{E}_{Q_t, Z} [\tilde{l}(\theta_t, Y_t)] + \frac{n\eta^2}{2\epsilon} \\ \Rightarrow \mathbb{E}_Z \left[\ln \left(\frac{W_{n+1}}{W_1} \right) \right] &\leq -\eta (\mathbb{E}_{QZ} [L(\theta, Y)] - n\beta\epsilon) + \frac{n\eta^2}{2\epsilon}. \end{aligned} \quad (26)$$

In the last step above, we have used (21). Combining (26) and (22) and rearranging the terms, we obtain

$$\mathbb{E}_{QZ} [L(\theta, Y)] - L(\theta^*, Y) \leq n\beta\epsilon + \frac{n\eta}{2\epsilon} + \frac{1}{\eta} \ln(1/\lambda_{\min}),$$

which is the regret R_n for HIL-N given by (18). \square

The bound in Theorem 6.1 neatly captures the effect of ϵ on the regret. Note that the term $n\beta\epsilon$ is a direct consequence of offloading sample t , when $Z_t = 1$. We denote the bound by

$$g(\epsilon, \eta) = n\beta\epsilon + \frac{n\eta}{2\epsilon} + \frac{1}{\eta} \ln(1/\lambda_{\min}). \quad (27)$$

We now minimize this bound and find the parameters that provide a bound that is sublinear in n .

LEMMA 6.2. *The function $g(\epsilon, \eta)$ defined in (27) has a global minimum at (ϵ^*, η^*) , where $\eta^* = \left(\frac{2 \ln^2(1/\lambda_{\min})}{\beta n^2} \right)^{1/3}$ and $\epsilon^* = \sqrt{\frac{\eta}{2\beta}}$. At this minimum, we have,*

$$g(\epsilon^*, \eta^*) = 3n^{2/3} \left(\frac{\beta \ln(1/\lambda_{\min})}{2} \right)^{1/3}.$$

PROOF. We can easily see the strict convexity of $g(\epsilon, \eta)$ in each dimension ϵ and η independently, which tells us that any inflection point of the function will be either a saddle point or a minima but not a maxima. We equate the

first-order partial derivatives to zero to get a set of points given by the equations

$$\frac{\partial g}{\partial \epsilon} = 0 \Rightarrow \epsilon = \sqrt{\frac{\eta}{2\beta}}, \quad (28)$$

$$\frac{\partial g}{\partial \eta} = 0 \Rightarrow \eta = \sqrt{\frac{2\epsilon \ln(1/\lambda_{\min})}{n}}. \quad (29)$$

However, it still remains to check if this point is unique and if this point is indeed a minimum, but not a saddle point. Seeing the uniqueness is straightforward by noting that these two expressions correspond to two non-decreasing, invertible curves in the ϵ - η plane, and thus they have a unique intersection. We find this intersection denoted using (ϵ^*, η^*) by substituting (28) in (29). We obtain

$$\eta^* = \sqrt{\frac{2\epsilon^* \ln(1/\lambda_{\min})}{n}} = \sqrt{\frac{2\sqrt{\eta^*/2\beta} \ln(1/\lambda_{\min})}{n}}.$$

We get η^* and ϵ^* by simplifying the above equation and then substituting it back in (28). Finally, to prove that (ϵ^*, η^*) is indeed a minimum, we verified that the determinant of the Hessian at (ϵ^*, η^*) is positive, the steps of which are not presented due to space constraints. Since (ϵ^*, η^*) is a unique minimum, it should be the global minimum. The proof is complete by substituting (ϵ^*, η^*) in (27). \square

Now, with the above Lemma in hand, we provide a sublinear regret bound for HIL-N in the following corollary.

COROLLARY 6.3. *With $\eta = \left(\frac{2\ln^2(1/\lambda_{\min})}{\beta n^2}\right)^{1/3}$ and $\epsilon = \min\{1, \sqrt{\frac{\eta}{2\beta}}\}$, HIL-N achieves a regret bound sublinear in n :*

$$R_n \leq 3n^{2/3} \left(\frac{\beta \ln(1/\lambda_{\min})}{2}\right)^{1/3}$$

PROOF. Note that, if $\sqrt{\frac{\eta}{2\beta}} \leq 1$, then $\epsilon = \sqrt{\frac{\eta}{2\beta}}$ and the results directly follows from Lemma 6.2. If $\sqrt{\frac{\eta}{2\beta}} > 1$, then we have $\epsilon = 1$. Substituting η value in $\sqrt{\frac{\eta}{2\beta}} > 1$, we obtain

$$\beta < \sqrt{\frac{\sqrt{2} \ln(1/\lambda_{\min})}{n}}. \quad (30)$$

Since $\epsilon = 1$, we will have $Z_t = 1$ for all t , i.e., HIL-N will always offload. Therefore, in this case, the total cost incurred by HIL-N is equal to $n\beta$. Now, using (30), we obtain

$$n\beta < \sqrt{\sqrt{2} \ln(1/\lambda_{\min})/n} = \sqrt{\sqrt{2}n \ln(1/\lambda_{\min})}.$$

Thus, when (30) holds and we have $\epsilon = 1$, the total cost itself is $O(n^{\frac{1}{2}})$ and therefore regret cannot be greater than $O(n^{\frac{1}{2}})$. The result follows by noting that $O(n^{\frac{2}{3}})$ is the larger bound. \square

Remarks: It is worth noting the following:

- (1) The proof steps in Theorem 5.1 closely follow some analysis of the standard EWF for PEA with the added complexity to account for the continuous experts and non-uniform discretization. The analysis for HIL-N is novel. In particular, the design of the unbiased estimator, steps 1 and 3 in the proof of Theorem 6.1, and the proof of Lemma 6.2 have new analysis.
- (2) The computational complexity of HIL-N is of the same order as that of HIL-F due to the similar interval generation steps.

- (3) We can remove the dependency of η on λ_{\min} and n by using a sequence of dynamic learning rates: $\eta_t = \frac{1}{\sqrt{t+1}}$. Sublinear regret bounds can be obtained for such a modification but we omit the analysis due to space constraints.

7 ALGORITHM IMPLEMENTATION AND COMPUTATIONAL COMPLEXITY

Recall from Lemma 4.1 that cumulative loss is a piece-wise constant function. We use this fact to compute the continuous domain integral in (6) efficiently by splitting the function into multiple rectangular areas of nonuniform base and then summing them up, where we do not make any discretization error but compute the exact value of the integral. In each round t , we increase the number of intervals by at most 1 as we split the interval containing p_t at p_t . After receiving p_t , we thus have $N \leq t + 1$ intervals with boundaries given by $p_{[0]} = 0$, $p_{[i]}$, $1 \leq i \leq t$, and $p_{[N]} = 1$. The weight $w_{i,t}$, $i \leq t + 1$ of the interval i in round t is then updated based on, 1) the weights in round $t - 1$, and 2) the position of the interval with respect to p_t . Note that in lines 12 of HIL-F and HIL-N, we state that the interval containing p_t should be split and in line 14 we state that the weights should be computed, but without giving more details. Below, we present four algorithmic rules that can be used to compute the probability q_t , interval boundaries $\{p_{[i]}\}$ and weights $\{w_{i,t}\}$, which needs to be computed in order. Let j be the interval strictly below p_t and dup be a boolean variable denoting duplicate p_t .

$$\begin{aligned}
(i) \quad j &\leftarrow \max\{i : p_{[i]} < p_t\}. \\
(ii) \quad dup &\leftarrow \text{FALSE}, \text{ if } p_\tau \neq p_t \forall \tau < t, \text{ TRUE otherwise.} \\
(iii) \quad q_t &\leftarrow \frac{\sum_{i=1}^j w_{i,t}(p_{[i]} - p_{[i-1]}) + w_{j+1,t}(p_t - p_{[j]})}{\sum_{i=1}^N w_{i,t}(p_{[i]} - p_{[i-1]})} \\
(iv) \quad N &\leftarrow \begin{cases} N & (dup = \text{TRUE}), \\ N + 1 & (dup = \text{FALSE}). \end{cases} \\
(v) \quad p_{[i]} &\leftarrow \begin{cases} p_{[i]} & i \leq j \text{ or } (dup = \text{TRUE}) \\ p_t & i = j + 1 \text{ and } (dup = \text{FALSE}) \\ p_{[i-1]} & j + 1 < i \leq N \text{ and } (dup = \text{FALSE}) \end{cases} \\
(vi) \quad w_{i,t} &\leftarrow \begin{cases} w_{i,t-1}e^{-\eta\beta} & p_{[i]} > p_t, (dup = \text{TRUE}) \\ w_{i-1,t-1}e^{-\eta\beta} & p_{[i]} > p_t, (dup = \text{FALSE}) \\ w_{i,t-1}e^{-\eta Y_t} & p_{[i]} \leq p_t, \text{HIL-F} \\ w_{i,t-1}e^{-\eta Y_t/\epsilon} & p_{[i]} \leq p_t, Z_t = 1, \text{HIL-N} \\ w_{i,t-1} & p_{[i]} \leq p_t, Z_t = 0, \text{HIL-N.} \end{cases}
\end{aligned}$$

In every round of computation, we need a certain constant number of additions, multiplications, and comparisons per interval, irrespective of the number of samples already processed. Thus, the computational complexity in each round is in the order of the number of intervals present in that interval. Now consider a set of n input images. In our proposed algorithms, the number of intervals in round t is upper bounded by $t + 1$. Thus, the worst-case computational complexity of HIL-F in round t is $O(t)$. Further, when λ_{\min} is the minimum difference between any two probabilities, the maximum number of intervals is clearly upper bounded by $1/\lambda_{\min}$, which reduces the complexity to $O(\min\{t, 1/\lambda_{\min}\})$.

PROPOSITION 1. *The computational complexity of HIL-F and HIL-N in round t is $O(\min\{t, 1/\lambda_{\min}\})$.*

Note that there can be many intervals with lengths larger than λ_{\min} , and thus the number of intervals can typically be less than $1/\lambda_{\min}$, which reduces the complexity in practice. As discussed earlier, one might approximate λ_{\min} to $1/n$ in some datasets, which gives us a complexity of $O(\min\{t, n\})$ in terms of the number of images. Also note that the above complexities are that of round t , and to get the total complexity of the algorithm, one has to sum it overall t .

Finally, we note that there can be datasets where $\lambda_{\min} < 1/n$ and for such cases the complexity from Proposition 1 will be $O(t)$. For instance, this is the case for the MNIST dataset but is not applicable for the Imagenette dataset with $\lambda_{\min} = \frac{1}{256}$. In this regard, we propose a practical modification to the algorithms by limiting the interval size to a minimum of $\Delta_{\min} > \lambda_{\min}$, where Δ_{\min} is a parameter chosen based on the complexity and cost tradeoffs. One then considers any different probabilities that lie within Δ_{\min} of each other as duplicates while generating new intervals in line 12 of HIL-F and HIL-N, which further reduces the complexity to $O(\min\{t, 1/\Delta_{\min}\})$. We observed by choosing different values of λ_{\min} (including $\frac{1}{n}$) that over a range of values, there is a notable reduction in algorithm runtime, with negligible difference in the expected average costs.

8 NUMERICAL RESULTS

In this section, we evaluate the performance of the proposed algorithms HIL-F and HIL-N by comparing them against each other as well as further benchmarks. Our evaluation scenario consists of two different classifiers and four different datasets. Firstly, we use 8-bit quantized MobileNet [14, 17], with width parameter 0.25, to classify the Imagenette and Imgewoof datasets [18]. We use 0.25 for the width parameter as it reduces the number of filters in each layer drastically, and the resulting MobileNet has a size of 0.5 MB, suitable to fit on an IoT sensor. Imagenette and Imgewoof are derived from Imagenet [9] and each contains a mixture of 10 different image classes with approximately 400 images per class. Out of the two, Imgewoof is a tougher dataset for classification as it contains 10 different breeds of dogs. Next, we use the test set of MNIST dataset [24], which contains 10000 images of handwritten digits from 0 through 9. For this dataset, we train a linear classifier (without regularizer), as the S-ML model. We convert the labels into vectors of size 10. For label l , i.e., digit l , we use all zero vectors except in l -th location, where the value is 1. After training the classifier, we scale the output to obtain a probability distribution over the 10 labels. The top-1 accuracy we obtain is 86%. Finally for CIFAR-10 [22, 23], we use a readily available trained CNN [13] with accuracy 84% as the S-ML model. Note that for all the simulations we invoke the assumption that the L-ML models have accuracy 1.

As explained in Section 3, we choose the expected average regret $\frac{1}{n}\mathbb{E}_Y[R_n]$ and expected average cost $\frac{1}{n}\mathbb{E}_{Y,\pi}[L(\theta, Y)]$ as the metrics to compare the performance. Recall that these metrics are upper bounded by 1, which is the maximum cost in a single round. For simplicity, we refer to them by average regret and average cost, respectively. For the simulations, we take 100 randomizations of the input sequence Y and for each of these randomizations we repeat the simulations 100 times. The randomization is for the statistical convergence across the sequences of Y (i.e., $\mathbb{E}_Y[\cdot]$), and the repetitions are for the convergence over the randomized decisions based on q_t made in line 4 of the algorithms (i.e., $\mathbb{E}_\pi[\cdot]$). We also checked with higher numbers of randomizations and repetitions and verified that 100×100 iterations are sufficient for statistical convergence. We use η and ϵ from (12) and Lemma 6.2, unless mentioned otherwise.

We use the following four baseline algorithms (i.e., policies) to compare the performance of HIL-F and HIL-N.

- (1) **Genie** – a non-causal policy, where only those images that are misclassified by S-ML are offloaded.
- (2) **θ^*** – an optimal fixed- θ policy. We compute this cost by running a brute-force grid search over all θ .
- (3) **Full offload** – all images are offloaded to the ES.

(4) **No offload** – all images are processed locally.

Before we go to the figures, we show the number of images offloaded and the number of images misclassified by different policies for the Imagenette dataset with a total of 3925 images in TABLE 2. These results are basically the data point with $\beta = 0.5$ from Fig. 3(a) (explained later). We can immediately infer from the table that HIL-F achieves an offloading rate and misclassification rate very close to that of the optimum fixed- θ policy. Further, HIL-F offloads approximately the same number of images as the optimum fixed- θ policy and achieves a top-1 accuracy of 92.3%. Contrast this with a much lower accuracy output of 43.2% by the chosen MobileNet as the S-ML. This also asserts that our framework with the cost structure β and Y indeed facilitates HI by reducing the number of offloaded images that are correctly classified by S-ML. Note that HIL-N also achieves high accuracy 95.2%, but it achieves this at the cost of offloading more images, 18% more than θ^* . This is because HIL-N can only get feedback from L-ML and chooses to offload more images to learn the best threshold. Note that a β of 0.5 corresponds to minimizing the sum of the total number of errors and offloads. One can see the optimum in this case visually from Fig. 2 in Section 1, where all images below the threshold and all misclassified images above the threshold add 1 to the total costs.

In Fig. 3, we compare the two proposed algorithms HIL-F and HIL-N with the baselines for all four datasets by plotting the average cost vs. β . Here, Fig. 3(a) through Fig. 3(d) correspond to Imagenette, Imagewoof, MNIST, and CIFAR-10 datasets, respectively. Observe that HIL-F performs very close to θ^* , having at most 6% higher total cost than θ^* among all four figures irrespective of the absolute value of the cost or the dataset considered. In Fig. 3(a) we have also added an inset where we have enlarged a portion of the figure to highlight the distinction between the proposed policies and θ^* . The vertical difference between these two corresponds to the corresponding regret. We can see that HIL-F achieves a cost very close to that of θ^* , having at most 4.5% higher total cost than θ^* throughout the range of β . For instance for the Imagenette dataset with $\beta = 0.5$, this increase is less than 1.4%. HIL-N on the other hand is more sensitive to the properties of the considered dataset. It performs much better than the Full offload policy and also follows a similar trend as that of the HIL-F. However, for larger values of β the comparative performance of HIL-N with the No offload policy deteriorates. This is because even when offloading is not optimum, HIL-N is offloading with a fixed probability $\epsilon > 0$, to learn the ground truth Y . Furthermore, we can see by comparing the four figures that, lower the accuracy of S-ML – for instance in Fig. 3(b) – larger will be the range of β for which HIL-N performs better than both No offload and Full offload policies.

In Fig. 4 we show the dependency of the algorithm on the learning rate parameter η plotting the average regret obtained by the proposed algorithms vs. the number of images for $\beta = 0.7$ and different values of η . We show the plots for theoretical bound-optimizing η , and for HIL-F we also show the plots with a few other η for comparison. First, note that the HIL-N learns slower compared to HIL-F which is an intuitive behavior because HIL-N cannot learn from those images that are not offloaded. Also, note that the difference in regret incurred by using $\hat{\lambda}_{\min} = 1/(n + 1)$ as an approximation of λ_{\min} is minimal – in the order 10^{-3} . Recall that the optimum η that we proposed is an optimum for the regret bound, but not necessarily for the regret itself. Hence, it is worth noting that, while using a larger η is slightly beneficial in this particular dataset, this turns out to be deleterious for the regret bound, which is valid for any

Images	Genie	Full offload	No offload	θ^*	HIL-F	HIL-N
offloaded	2230	3925	0	2588	2626	3056
Misclassified	0	0	2230	303	304	191

Table 2. Number of images offloaded and misclassified for different policies on Imagenette with $\beta = 0.5$ and optimal η, ϵ .

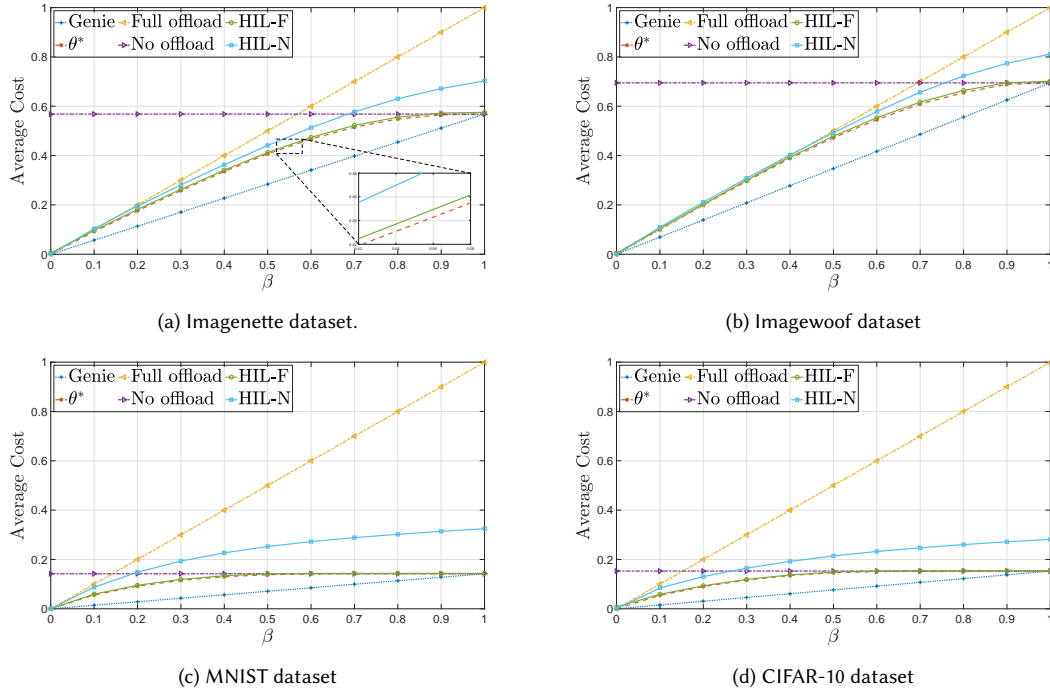


Fig. 3. Average cost incurred by various offloading policies vs. β for different datasets. The bound optimizing η and ϵ are used assuming a prior knowledge of λ_{\min} . Note that the curves corresponding to θ^* and HIL are very close to each other.

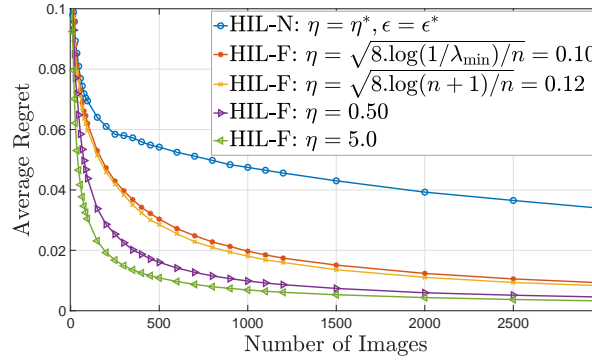


Fig. 4. Average regret vs. Number of images for $\beta = 0.7$ using HIL-F and HIL-N on the imagenette database with various η .

given dataset. Further, too large an η will give too large weights to the thresholds that achieved lower costs in the past, making the algorithm resemble a deterministic algorithm that cannot guarantee performance [6].

9 CONCLUSION

We considered an ED embedded with S-ML and an ES having L-ML and explored the idea of HI, where the ED can benefit from only offloading samples for which S-ML outputs incorrect inference. Since an ideal implementation of HI is infeasible, we proposed a novel meta-learning framework where the ED decides to offload or not to offload after observing the maximum probability p in the probability mass function output by S-ML. For the full feedback scenario, we proposed HIL-F, which assigns exponential weights to decision thresholds $\theta \in [0, 1]$ based on past costs and probabilistically chooses a threshold, based on p , to offload or not. For the no-local feedback scenario, we proposed HIL-N, which uses an unbiased estimator of the cost and generates an additional Bernoulli random variable Z and always offloads if $Z = 1$. A novel and unique aspect of the proposed algorithms is that we use non-uniform discretization, i.e., create new intervals in each round based on p and use these intervals as experts. We proved that HIL-F and HIL-N have sublinear regret bounds $\sqrt{n \ln(1/\lambda_{\min})/2}$ and $O\left(n^{2/3} \ln^{1/3}(1/\lambda_{\min})\right)$, respectively, and have runtime complexity $O(\min\{t, 1/\lambda_{\min}\})$ in round t . Here, it is worth noting that the term $1/\lambda_{\min}$ acts similarly to the number of experts in PEA as far as regret bounds are concerned and we have explained simple methods to approximate it. For verifying the results, we generated values of p for four datasets, namely, Imagenette, Imagewoof, MNIST, and CIFAR-10, and compared the performance of HIL-F and HIL-N with four different baseline policies, including the *fixed- θ* policy. The cost achieved by the proposed algorithms is always lower compared to the *Full offload* and the *No offload* policies and is close to the cost achieved by the optimum fixed- θ policy for a wide range of β . More importantly, the algorithms achieve much higher accuracy compared to S-ML while offloading a marginally higher number of images compared to the optimum fixed- θ policy.

REFERENCES

- [1] Peter Auer, Ronald Ortner, and Csaba Szepesvári. 2007. Improved Rates for the Stochastic Continuum-Armed Bandit Problem. In *Learning Theory*, Nader H. Bshouty and Claudio Gentile (Eds.). Springer Berlin Heidelberg, 454–468.
- [2] Sébastien Bubeck. 2011. Introduction to online optimization. (2011).
- [3] Sébastien Bubeck and Nicolò Cesa-Bianchi. 2012. Regret Analysis of Stochastic and Nonstochastic Multi-armed Bandit Problems. *Foundations and Trends® in Machine Learning* 5, 1 (2012), 1–122. <https://doi.org/10.1561/22000000024>
- [4] Sébastien Bubeck, Rémi Munos, Gilles Stoltz, and Csaba Szepesvári. 2011. X-Armed Bandits. *J. Mach. Learn. Res.* 12, null (jul 2011), 1655–1695.
- [5] Nicolò Cesa-Bianchi, Yoav Freund, David Haussler, David P. Helmbold, Robert E. Schapire, and Manfred K. Warmuth. 1997. How to Use Expert Advice. *J. ACM* 44, 3 (may 1997), 427–485. <https://doi.org/10.1145/258128.258179>
- [6] Nicolò Cesa-Bianchi and Gábor Lugosi. 2006. *Prediction, learning, and games*. Cambridge University Press. I–XII, 1–394 pages.
- [7] N. Cesa-Bianchi, G. Lugosi, and G. Stoltz. 2005. Minimizing regret with label efficient prediction. *IEEE Transactions on Information Theory* 51, 6 (2005), 2152–2162. <https://doi.org/10.1109/TIT.2005.847729>
- [8] Eduardo Cuervo, Aruna Balasubramanian, Dae ki Cho, Alec Wolman, Stefan Saroiu, Ranveer Chandra, and Paramvir Bahl. 2010. MAUI: making smartphones last longer with code offload. In *MobiSys*. ACM, 49–62.
- [9] Jia Deng, Wei Dong, Richard Socher, Li-Jia Li, Kai Li, and Li Fei-Fei. 2009. Imagenet: A large-scale hierarchical image database. In *Proc. IEEE CVPR*. 248–255.
- [10] Lei Deng, Guoqi Li, Song Han, Luping Shi, and Yuan Xie. 2020. Model Compression and Hardware Acceleration for Neural Networks: A Comprehensive Survey. *Proc. IEEE* 108, 4 (2020), 485–532. <https://doi.org/10.1109/JPROC.2020.2976475>
- [11] Emily Denton, Wojciech Zaremba, Joan Bruna, Yann LeCun, and Rob Fergus. 2014. Exploiting Linear Structure within Convolutional Networks for Efficient Evaluation. In *Proc. NeurIPS*. 1269–1277.
- [12] Andrea Fresa and Jaya Prakash Champati. 2021. Offloading Algorithms for Maximizing Inference Accuracy on Edge Device Under a Time Constraint. *CoRR* abs/2112.11413 (2021). <https://arxiv.org/abs/2112.11413>
- [13] GitHub Repository. 2021. Retrieving the predictions in the CIFAR-10 dataset. Retrieved January 26, 2023 from https://github.com/TracyRenee61/CIFAR_10/blob/main/CIFAR10_PyTprch_83_accuracy.ipynb
- [14] GitHub Repository, Keras.io. 2022. Retrieved January 26, 2023 from <https://keras.io/api/applications/mobilenet/>
- [15] Songtao Guo, Jiadi Liu, Yuanyuan Yang, Bin Xiao, and Zhetao Li. 2019. Energy-Efficient Dynamic Computation Offloading and Cooperative Task Scheduling in Mobile Cloud Computing. *IEEE Transactions on Mobile Computing* 18, 2 (2019), 319–333. <https://doi.org/10.1109/TMC.2018.2831230>

- [16] Song Han, Jeff Pool, John Tran, and William J. Dally. 2015. Learning Both Weights and Connections for Efficient Neural Networks. In *Proc. NeurIPS*. 1135–1143.
- [17] Andrew G. Howard, Menglong Zhu, Bo Chen, Dmitry Kalenichenko, Weijun Wang, Tobias Weyand, Marco Andreetto, and Hartwig Adam. 2017. MobileNets: Efficient Convolutional Neural Networks for Mobile Vision Applications. *CoRR* abs/1704.04861 (2017). arXiv:1704.04861
- [18] Jeremy Howard and Sylvain Gugger. 2020. Fastai: A Layered API for Deep Learning. *Information* 11, 2 (2020). <https://github.com/fastai/imagenette>
- [19] Chuang Hu, Wei Bao, Dan Wang, and Fengming Liu. 2019. Dynamic Adaptive DNN Surgery for Inference Acceleration on the Edge. In *IEEE INFOCOM 2019 - IEEE Conference on Computer Communications*. 1423–1431. <https://doi.org/10.1109/INFOCOM.2019.8737614>
- [20] Chenghao Hu and Baochun Li. 2022. Distributed Inference with Deep Learning Models across Heterogeneous Edge Devices. In *Proc. IEEE INFOCOM*. 330–339. <https://doi.org/10.1109/INFOCOM48880.2022.9796896>
- [21] Yiping Kang, Johann Hauswald, Cao Gao, Austin Rovinski, Trevor Mudge, Jason Mars, and Lingjia Tang. 2017. Neurosurgeon: Collaborative Intelligence Between the Cloud and Mobile Edge. In *in Proc. ASPLOS*. Association for Computing Machinery, 615–629. <https://doi.org/10.1145/3037697.3037698>
- [22] Alex Krizhevsky. 2009. The CIFAR-10 dataset. Retrieved January 26, 2023 from <https://www.cs.toronto.edu/~kriz/cifar.html>
- [23] Alex Krizhevsky, Geoffrey Hinton, et al. 2009. Learning multiple layers of features from tiny images. (2009).
- [24] Yann LeCun and Corinna Cortes. 2010. MNIST handwritten digit database. <http://yann.lecun.com/exdb/mnist/>. (2010). <http://yann.lecun.com/exdb/mnist/>
- [25] En Li, Liekang Zeng, Zhi Zhou, and Xu Chen. 2020. Edge AI: On-Demand Accelerating Deep Neural Network Inference via Edge Computing. *IEEE Transactions on Wireless Communications* 19, 1 (2020), 447–457. <https://doi.org/10.1109/TWC.2019.2946140>
- [26] Ivana Nikoloska and Nikola Zlatanov. 2021. Data Selection Scheme for Energy Efficient Supervised Learning at IoT Nodes. *IEEE Communications Letters* 25, 3 (2021), 859–863. <https://doi.org/10.1109/LCOMM.2020.3034992>
- [27] Samuel S. Ogden and Tian Guo. 2020. MDINFERENCE: Balancing Inference Accuracy and Latency for Mobile Applications. In *Proc. IEEE IC2E*. 28–39. <https://doi.org/10.1109/IC2E48712.2020.00010>
- [28] Mohammad Rastegari, Vicente Ordonez, Joseph Redmon, and Ali Farhadi. 2016. XNOR-Net: ImageNet Classification Using Binary Convolutional Neural Networks. In *Computer Vision – ECCV 2016*, Bastian Leibe, Jiri Matas, Nicu Sebe, and Max Welling (Eds.). Springer International Publishing, Cham, 525–542.
- [29] Ramon Sanchez-Iborra and Antonio F. Skarmeta. 2020. TinyML-Enabled Frugal Smart Objects: Challenges and Opportunities. *IEEE Circuits and Systems Magazine* 20, 3 (2020), 4–18. <https://doi.org/10.1109/MCAS.2020.3005467>
- [30] Mahadev Satyanarayanan, Paramvir Bahl, Ramon Caceres, and Nigel Davies. 2009. The Case for VM-Based Cloudlets in Mobile Computing. *IEEE Pervasive Computing* 8, 4 (2009), 14–23. <https://doi.org/10.1109/MPRV.2009.82>
- [31] Shashank Singh. 2021. Continuum-Armed Bandits: A Function Space Perspective. In *Proceedings of The 24th International Conference on Artificial Intelligence and Statistics (Proceedings of Machine Learning Research, Vol. 130)*, Arindam Banerjee and Kenji Fukumizu (Eds.). PMLR, 2620–2628.
- [32] Sowndarya Sundar, Jaya Prakash Varma Champati, and Ben Liang. 2020. Multi-user Task Offloading to Heterogeneous Processors with Communication Delay and Budget Constraints. *IEEE Transactions on Cloud Computing* (2020), 1–1. <https://doi.org/10.1109/TCC.2020.3019952>
- [33] Ben Taylor, Vicent Sanz Marco, Willy Wolff, Yehia Elkhatib, and Zheng Wang. 2018. Adaptive Deep Learning Model Selection on Embedded Systems. *SIGPLAN Not.* 53, 6 (jun 2018), 31–43. <https://doi.org/10.1145/3299710.3211336>
- [34] Surat Teerapittayanon, Bradley McDanel, and H.T. Kung. 2016. BranchyNet: Fast inference via early exiting from deep neural networks. In *Proc. ICPR*. 2464–2469.
- [35] Junjue Wang, Ziqiang Feng, Zhuo Chen, Shilpa George, Mihir Bala, Padmanabhan Pillai, Shao-Wen Yang, and Mahadev Satyanarayanan. 2018. Bandwidth-Efficient Live Video Analytics for Drones Via Edge Computing. In *2018 IEEE/ACM Symposium on Edge Computing (SEC)*. 159–173. <https://doi.org/10.1109/SEC.2018.00019>
- [36] Junjue Wang, Ziqiang Feng, Zhuo Chen, Shilpa Anna George, Mihir Bala, Padmanabhan Pillai, Shao-Wen Yang, and Mahadev Satyanarayanan. 2019. Edge-Based Live Video Analytics for Drones. *IEEE Internet Computing* 23, 4 (2019), 27–34. <https://doi.org/10.1109/MIC.2019.2909713>
- [37] Xiaofei Wang, Yiwen Han, Victor C. M. Leung, Dusit Niyato, Xueqiang Yan, and Xu Chen. 2020. Convergence of Edge Computing and Deep Learning: A Comprehensive Survey. *IEEE Communications Surveys and Tutorials* 22, 2 (2020), 869–904. <https://doi.org/10.1109/COMST.2020.2970550>
- [38] Zizhao Wang, Wei Bao, Dong Yuan, Liming Ge, Nguyen H. Tran, and Albert Y. Zomaya. 2019. SEE: Scheduling Early Exit for Mobile DNN Inference during Service Outage. In *in Proc. MSWIM*. 279–288. <https://doi.org/10.1145/3345768.3355917>
- [39] Mitchell Wortsman, Gabriel Ilharco, Samir Ya Gadre, Rebecca Roelofs, Raphael Gontijo-Lopes, Ari S Morcos, Hongseok Namkoong, Ali Farhadi, Yair Carmon, Simon Kornblith, and Ludwig Schmidt. 2022. Model soups: averaging weights of multiple fine-tuned models improves accuracy without increasing inference time. In *Proceedings of the 39th International Conference on Machine Learning (Proceedings of Machine Learning Research, Vol. 162)*. PMLR, 23965–23998.

This figure "sample-franklin.png" is available in "png" format from:

<http://arxiv.org/ps/2304.00891v1>